Progress in Physics of Applied Materials 5 (2025), Serial Number 9, 217 – 222

Semnan University

Progress in Physics of Applied Materials

journal homepage: https://ppam.semnan.ac.ir/

Investigation on the Electronic Properties of Functionalized MXene Nanoribbons M_2XT_2 (M=Ti, Zr, Sc & X=C & T=O, F) with Zigzag Edges

Mahdi Shirazinia [a], **Edris Faizabadi** [a*]

[a] *School of Physics, Iran University of Science and Technology, Tehran, Iran*

ARTICLE INFO

Article history:
Received: 13 September 2024
Revised: 21 December 2024
Accepted: 3 January 2025
Published online: 12 August 2025

Keywords:
MXenes, Nanoribbons;
Zigzag Edges;
Electronic Properties;
Density Functional Theory.

ABSTRACT

Nanoribbons, due to their unique quantum confinement effects and surface effects, have high potential for applications in nanoelectronics and spintronics. This study investigates the electronic properties of zigzag-edged MXene nanoribbons, focusing on functionalized MXenes of the form M_2XT_2, where M = Ti, Zr, Sc, X = C, and T = O, F. Using density functional theory (DFT), we analyze nanoribbons with varying sizes (n = 9 to 15) and edge configurations. Our results reveal that except for 9-ZNR, 12-ZNR, and 15-ZNR, all other zigzag-edged MXene nanoribbons exhibit metallic properties, with the presence of X = C in the edge configurations being a distinguishing factor. For the semiconducting nanoribbons, the band gaps decrease uniformly with increasing width, which aligns with quantum confinement effects. We also observe that the conduction and valence bands are primarily influenced by the d-orbitals of the transition metals (Ti, Zr, Sc) and the p-orbitals of the functional groups (C, O, F), with specific band structures indicating indirect band gaps for semiconductor behavior. Our findings suggest that the electronic properties of these nanoribbons are significantly affected by their size, edge configuration, and functionalization, providing valuable insights for potential applications in electronic and optoelectronic devices.

1. Introduction

Two-dimensional materials have attracted significant attention due to their unique properties and potential for diverse applications. By confining two-dimensional materials, one can create one-dimensional structures such as nanoribbons and nanotubes, which exhibit vastly different physical properties compared to their two-dimensional counterparts due to quantum confinement and surface effects[1]. For example, two-dimensional graphene, which has been extensively studied, is a semimetal, whereas one-dimensional graphene nanoribbons can be semiconductors with a bandgap that can be tuned as a function of the ribbon width and edge configuration (armchair versus zigzag)[2]. Studies on similar nanoribbons with a honeycomb structure derived from two-dimensional silicene[3], boron nitride[4], and transition metal dichalcogenides[5] have also demonstrated interesting size- and edge-dependent properties in these one-dimensional nanostructures. Some of the aforementioned nanoribbons have been fabricated using methods such as lithography, bottom-up synthesis, and nanotube unzipping[6, 7].

Recently, a new class of two-dimensional materials known as MXenes has attracted significant attention due to their outstanding properties, such as high damage tolerance, resistance to oxidation, and excellent electrical and thermal conductivity[8]. These materials can be functionalized for new physical and chemical applications. Experimentally, MXenes are synthesized from bulk MAX phases through exfoliation. MAX phases are a large family of layered, hexagonal carbides and nitrides with the general formula $M_{n+1}AX_n$, where n ranges from 1 to 3, M is an early transition metal, A is a group A element (mainly from groups IIIA and IVA), and X is carbon and/or

* Corresponding author. Tel.: +98-2173225882
E-mail address: edris@iust.ac.ir

Cite this article as:

Shirazinia M. and Faizabadi E., 2025. Investigation on the Electronic Properties of functionalized MXene Nanoribbons M_2XT_2 (M=Ti, Zr, Sc & X=C & T=O, F) with Zigzag Edges. *Progress in Physics of Applied Materials*, *5*(2), pp.217-222. DOI: **10.22075/PPAM.2025.35320.1116**

nitrogen[9]. MXenes are obtained by removing the A layer from MAX phases using various methods, and their surfaces often tend to chemically react with functional groups such as O, F, and OH, resulting in functionalization. Therefore, the formula of pure MXenes is $M_{n+1}X_n$, while the formula of functionalized MXenes is $M_{n+1}X_nT_2$, where T represents the terminating functional groups. The functionalization of MXenes significantly affects their properties, particularly their electronic properties. For example, while all pure MXenes are metallic, after functionalization, some of the thinnest MXenes, such as Ti_2CO_2, Zr_2CO_2, Hf_2CO_2, Sc_2CO_2, Sc_2CF_2, and $Sc_2C(OH)_2$, become semiconductors with bandgaps ranging from 0.24 to 1.8 electron volts[10]. Therefore, the study of MXene functionalization is a highly intriguing topic for current research.

Several first-principles studies on various MXene nanoribbons have been conducted to date. Zhao et al. examined the electronic properties of Ti_2C, Ti_3C_2, and V_2C nanoribbons in both bare and oxygen-functionalized forms at different sizes[11]. Zhang et al. explored the carrier mobility of Ti_2CO_2 nanoribbons[12]. Additionally, Hong et al. provided extensive research and findings on a wide range of terminated MXene nanoribbons derived from 2D monolayers with the composition M2XT2[13]. In this study, we first focus on fabricating zigzag-edged nanoribbons of varying sizes from selected two-dimensional materials, namely the functionalized MXenes Ti_2CO_2, Zr_2CO_2, and Sc_2CF_2. We then investigate their electronic properties using density functional theory. This study will reveal that the edge effects of nanoribbons have a significant impact on their electronic properties.

2. Computational Methods and Models

All calculations were performed using density functional theory, implemented through the Quantum ESPRESSO software package[14-16]. All simulations in this study were carried out using the XCrySDen software[17]. The calculations utilize the SSSP PBE Precision v1.3.0 pseudopotentials, available on the Materials Cloud website[18]. For the calculations of zigzag-edged MXene nanoribbons, a kinetic energy cutoff of 45 Ry for wave functions and a charge density cutoff of 450 Ry are used. The energy cutoff specifies the extent of kinetic energy included in the plane waves of electronic wave functions in DFT calculations, while the charge density cutoff is a parameter used for expanding the electronic charge density. The chosen values in this paper are quite reasonable and even exceed those used in previous studies on nanoribbons for increased accuracy[11]. Additionally, the spin of the particles is also considered and incorporated into the calculations.

For the functionalization of the selected two-dimensional MXenes, three configurations are considered. Assuming that the functional groups oxygen and fluorine are represented as T, and the atoms Ti, Zr, and Sc are denoted as M, with carbon as X, the configurations are as follows: In the first configuration, T atoms in the lower layer are positioned directly beneath the M atoms in the upper layer, while T atoms in the upper layer are directly above the M atoms in the lower layer. In the second configuration, T atoms in the upper (or lower) layer are positioned above (or below) the X atoms. The third configuration combines the first and second configurations, with T atoms in the lower layer placed under the X atoms and T atoms in the upper layer placed directly above the M atoms in the lower layer[13]. Hong and colleagues investigated the functionalization of several MXenes with these three configurations and reported the most stable configuration, which had the lowest total energy among the others. The three MXenes selected in this study all exhibit the lowest energy and most stable state in the first configuration; thus, the first configuration is used for the functionalization of MXenes in this paper[13]. As mentioned, MXenes are cut into nanoribbons of various directions and sizes. The selected MXenes in this study all have a hexagonal lattice, and thus, the nanoribbons will have two well-known edge types: armchair and zigzag, in various sizes. The method of cutting the nanoribbons from their corresponding two-dimensional materials is illustrated in Figure 1. As shown in Figure 1, the resulting nanoribbons with zigzag and armchair edges are designated by size parameters n_z and n_a, respectively. In this study, only nanoribbons with zigzag edges are examined and are referred to as n_z-ZNR.

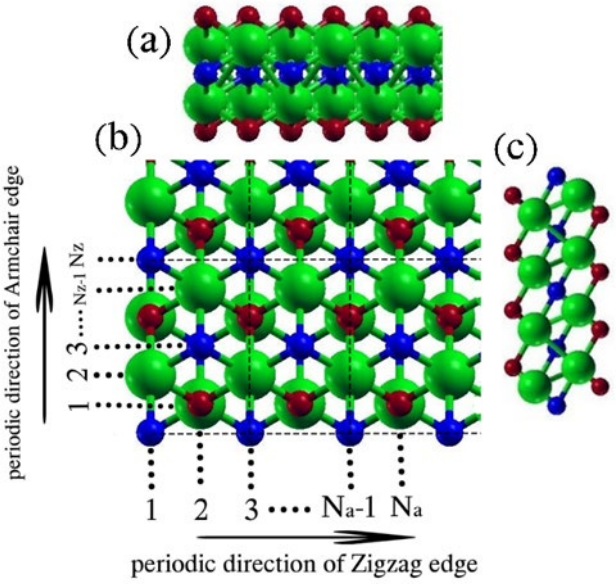

Fig. 1. (a) and (c) side views, and (b) the top view of M_2XT_2 nanoribbons. The elements M, X, and T are represented in green, blue, and red, respectively.

Classifying ZNRs is challenging because they exhibit two different types of atomic rows extending periodically. These atomic rows consist of rows of M and T atoms (with M atoms either above or below T atoms, referred to collectively as M) or rows of X atoms. When cutting the corresponding two-dimensional material into zigzag-edged nanoribbons of various sizes, we find six types of edges with different sizes. The naming convention for these types follows previous studies [11, 13], where the arrangement of atomic rows in ZNRs can be represented as ...MMXMMX..., leading to three types of edges: MMX, MXM, and XMM, with the first letter indicating the outermost atomic row. Considering all combinations of edge types at the start and end, six types of ZNR structures can be obtained:(1) n_z- (MMX-MMX)-ZNR, where n_z=3p (p is a positive integer), representing ZNRs with size n_z and two

MMX and XMM edges (the same as MMX if read from the top); (2) n_z- (MXM-MXM)-ZNR, where n_z=3p; (3) n_z- (MMX-MXM)-ZNR, where n_z = 3p + 1; (4) n_z- (XMM-MMX)-ZNR, where nz = 3p + 1; (5) n_z- (MMX-XMM)-ZNR, where n_z = 3p + 2; (6) n_z- (MXM-MMX)-ZNR, where n_z = 3p + 2. According to previous studies, the MMX-MMX, MMX-MXM, and MMX-XMM structures exhibit the highest binding energies, indicating that they are more stable compared to the other structures[11]. Therefore, in this paper, we consider these three structures for ZNRs, with the lower edge of the nanoribbons being MMX. As previously mentioned, the three edge types MMX, MXM, and XMM are present on the upper edge, allowing for the construction of all sizes with these edges. Since the edge of ZNR nanoribbons is determined by the atomic composition and arrangement of the three outer atomic rows, and because ZNR nanoribbons with n_z less than 9 undergo significant structural changes after optimization due to their comparable width and thickness, this study focuses on sizes ranging from 9 to 15, as illustrated in Figure 1[13]. According to the provided details, sizes 9, 12, and 15 have MMX-MMX edges, sizes 10 and 13 have MMX-MXM edges, and sizes 11 and 14 have MMX-XMM edges. For brevity, only the size will be mentioned from now on. In this study, the periodic direction for all nanoribbons is aligned along the z-axis in the Cartesian system for simulation purposes. To prevent interactions from periodic images, the nanoribbons are separated by 20 Å along the non-periodic directions (x and y), creating a large vacuum space. The Broyden–Fletcher–Goldfarb–Shanno (BFGS) method is used to optimize the nanoribbons along the z-direction (the periodic direction). Calculations are performed with an energy convergence criterion of 10^{-7} Ry between successive self-consistent iterations. The Brillouin zone is sampled using a Monkhorst–Pack grid of 1×1×18 for structural optimization and self-consistent calculations of the nanoribbons. For greater accuracy, after structural optimization and self-consistent calculations, the density of states and other electronic properties are determined using a denser grid of 1×1×36 in subsequent non-self-consistent calculations.

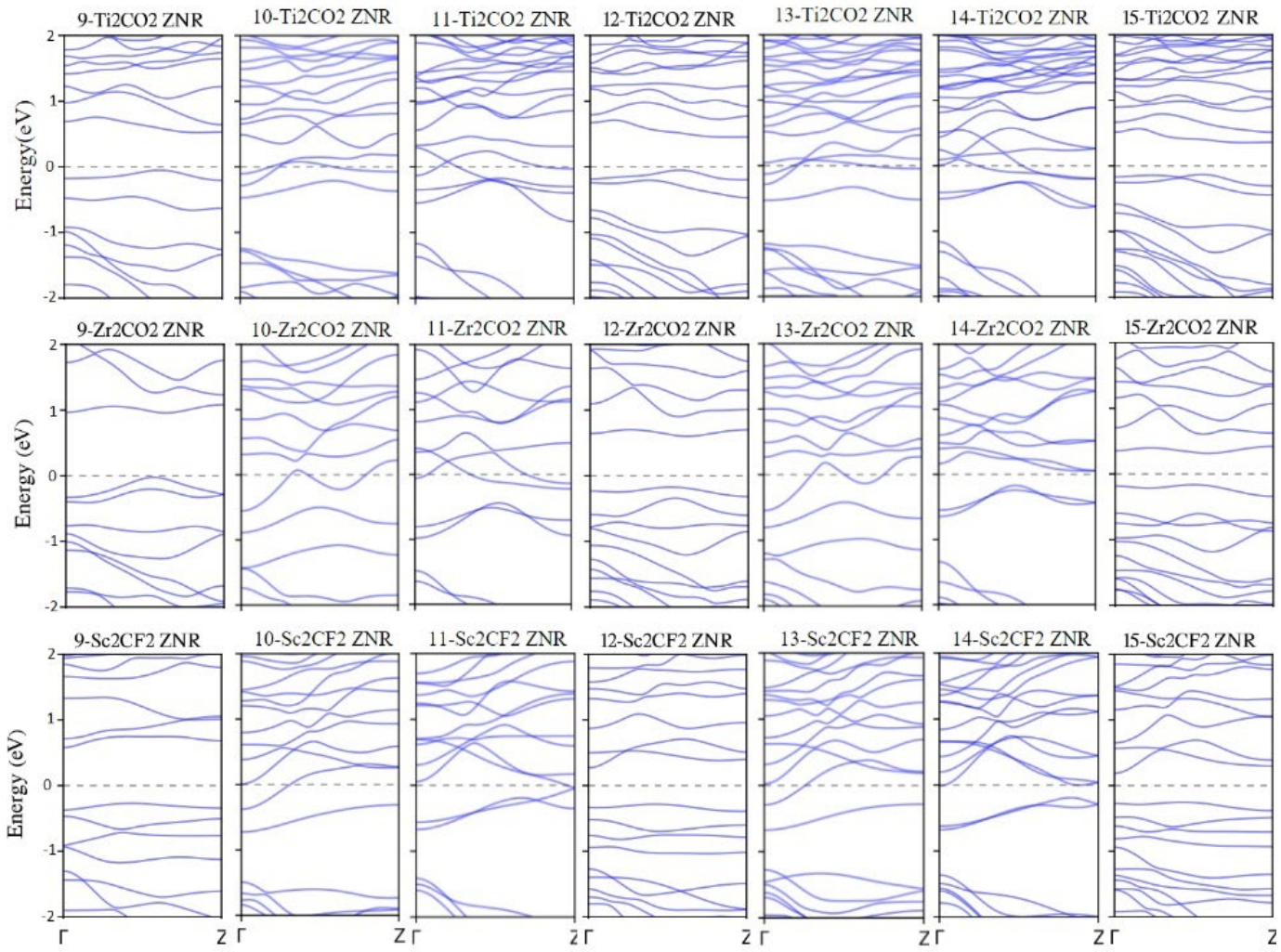

Fig. 2. Band structures of semiconducting MZNRs. The Fermi energy is adjusted to zero

3. Results and Discussion

As mentioned, this study considers three different types of functionalized two-dimensional MXenes (Ti_2CO_2, Zr_2CO_2, and Sc_2CF_2), with the goal of creating one-dimensional zigzag-edged nanoribbons associated with them. As an initial step, we calculate the lattice parameters for these two-dimensional structures. The optimized lattice

parameters are found to be 3.04 Å, 3.31 Å, and 3.29 Å for Ti_2CO_2, Zr_2CO_2, and Sc_2CF_2, respectively. These values are in good agreement with previous theoretical findings[13]. As noted earlier, zigzag-edged MXene nanoribbons (MZNR) with varying widths have been constructed from the two-dimensional MXenes. The width parameter, n_z, ranges from 9 to 15, as shown in Figure 1.

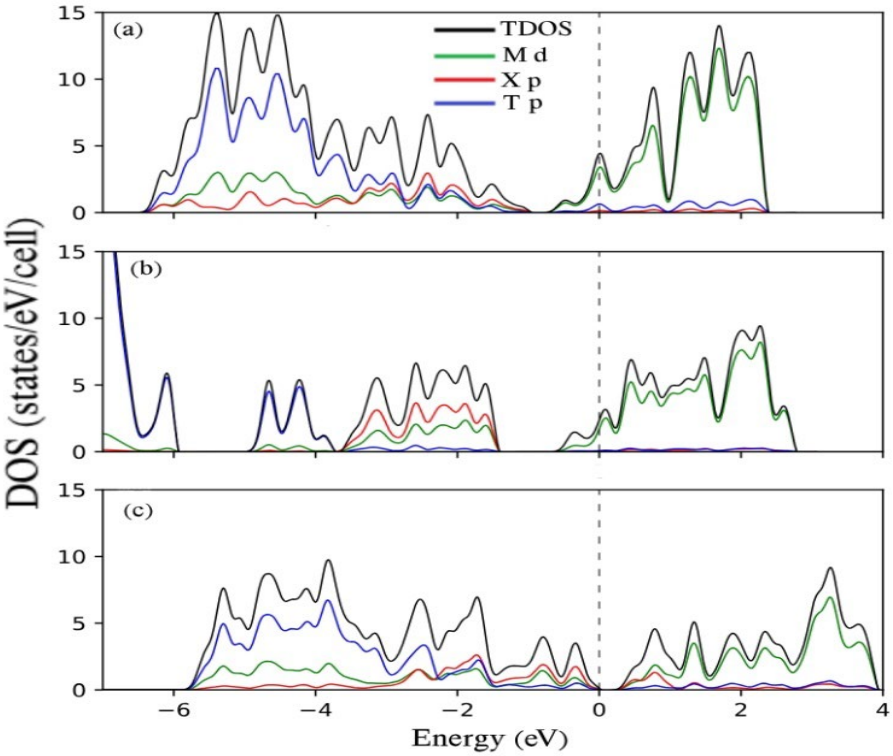

Fig. 3. TDOS and PDOS on selected atomic orbitals of (a)11-Ti2CO2 ZNR, (b)10-Sc2CF2 ZNR, and (c)semiconducting 9-Zr_2CO_2 ZNR. The Fermi energy is adjusted to zero

Analysis shows that all selected zigzag-edged MXene nanoribbons (MZNR), except for ZNR-9, ZNR-12, and ZNR-15, exhibit metallic properties. The distinguishing factor among the 9Z, 12Z, and 15Z configurations compared to other MZNRs is the presence of X=C in the n-th row of these semiconducting MXenes, as illustrated in Figure 1. In contrast, metallic zigzag-edged MXene nanoribbons contain M elements or a combination of M and T elements in the n-th row. This difference in elemental composition relates to the observed semiconductor or metallic properties in MZNRs. Figure 2 shows the band structure of the functionalized zigzag-edged MXene nanoribbons. The band gaps for 9-ZTi_2CO_2, 12-ZTi_2CO_2, 15-ZTi_2CO_2, 9-ZZr_2CO_2, 12-ZZr_2CO_2, 15-ZZr_2CO_2, 9-ZSc_2CF_2, 12-ZSc_2CF_2, and 15-ZSc_2CF_2 are 0.57 eV, 0.50 eV, 0.48 eV, 0.98 eV, 0.77 eV, 0.47 eV, 0.85 eV, 0.55 eV, and 0.44 eV, respectively. The band gaps decrease uniformly with increasing width of the nanoribbons. This observed trend can be explained by the quantum confinement effect. For more discussion, we note that with the increase in the width of semiconducting ZNRs, it is expected that their band gaps will move toward their corresponding 2D band gaps. As mentioned in Section 1, Ti_2CO_2, Zr_2CO_2, and Sc_2CF_2 are semiconductors with band gaps of 0.32, 0.97, and 1.03, respectively[13]. In the case of semiconducting ZNRs of Ti_2CO_2, the convergence of the band gaps towards the band gap of 2D Ti_2CO_2 is evident, and the calculated band gaps in this paper converge towards 0.32, which has also been reported in previous studies [13]. However, this phenomenon is not observed in the calculated band gaps of semiconducting ZNRs of Zr_2CO_2 and Sc_2CF_2. Previous investigation of the wave-function characteristics for the valence and conduction bands near the band gap of these semiconducting ZNRs reveals that edge states generally emerge at the CBM, while the VBM remains bulklike, with filled edge states found down the valence band[13, 19]. The presence of edge states can modify the electronic band structure of a material, potentially leading to a reduction in the band gap. This is because edge states can introduce new energy levels within the band gap, effectively narrowing it. For example, in graphene, edge states at zigzag edges can introduce localized states within the band gap, which can alter the electronic properties of the material[20, 21]. The conduction band minimum (CBM) and valence band maximum (VBM) for these semiconductors are located between the Γ and Z points, except for the CBM of the zigzag-edged semiconducting Sc_2CF_2 nanoribbons, which is situated at the Γ point. this exception can be a reason for the existence of edge states at this point. The presence of these indirect band gaps is crucial for the semiconductor behavior in devices utilizing these nanoribbons.

Figure 3 shows the total density of states (TDOS) and the partial density of states (PDOS) for selected nanoribbons. In all samples, the conduction band and the Fermi level are primarily derived from the d-orbital states of Ti, Zr, and Sc elements, while the valence band states, ranging from -7 to 0 eV, are divided into two sub-bands. In the Ti_2CO_2 ZNR and Zr_2CO_2 ZNR nanoribbons, the first sub-band, within the approximate range of -3 to 0 eV, is nearly equally composed of d-orbital states of Ti and Zr, and p-

orbitals of carbon and oxygen (with a greater contribution from carbon p-orbitals). The second sub-band, within the approximate range of -6 to -3 eV, is mainly made up of p-orbitals of oxygen, with some contribution from the d-orbital states of Ti and Zr due to strong hybridization between them. For the semiconducting Sc_2CF_2 ZNRs, these sub-bands are distinctly separated, with two sub-bands being separated by a small gap (approximately 1 eV). The first sub-band, within the approximate range of -3.5 to 0 eV, is almost equally composed of Sc d-orbital states and carbon p-orbitals (with a greater contribution from carbon p-orbitals), while the second sub-band, within the approximate range of -7 to -4.6 eV, is predominantly dominated by fluorine p-orbitals. This type of orbital contribution in selected semiconductor compositions is logical, as the electronic configuration of the involved elements and their tendency to achieve a stable noble gas configuration dictate this behavior. In the selected compounds, namely Ti_2CO_2, Zr_2CO_2, and Sc_2CF_2, the elements Ti, Zr, and Sc donate their valence electrons to the elements C, O, and F. Consequently, the d-orbitals of Ti, Zr, and Sc, which usually play a more significant role than their other orbitals, become vacant and the p-orbitals of C, O, and F are filled, leading all elements to achieve a stable noble gas configuration before or after. Thus, the conduction band is predominantly derived from the d-orbital states of Ti, Zr, and Sc, while the valence states mainly originate from the p-orbital states of C, O, and F.

4. Conclusions

In this study, we have explored the electronic properties of zigzag-edged MXene nanoribbons, focusing on Ti_2CO_2, Zr_2CO_2, and Sc_2CF_2. The results demonstrate a clear distinction between metallic and semiconducting behaviors based on the edge configurations and the presence of carbon in the edge rows. The decrease in band gaps with increasing nanoribbon width, observed as a consequence of quantum confinement effects, highlights the tunable nature of these materials. The detailed analysis of the density of states indicates that the electronic behavior is predominantly influenced by the d-orbitals of the transition metals and the p-orbitals of the functional groups. These findings not only deepen our understanding of the fundamental electronic properties of MXene nanoribbons but also open avenues for tailoring these properties for specific applications in electronic and optoelectronic devices. The study underscores the importance of edge configuration and functionalization in determining the electronic characteristics of MXenes, offering a pathway for designing advanced materials with desired electronic properties.

Acknowledgements

This work was supported by Iran University of Science and Technology (IUST) Grant No. 160/20793.

Conflicts of interest

The authors declare that they have no known competing financial interests or personal relationships that could have appeared to influence the work reported in this paper.

Authors contribution statement

M. Shirazinia: Simulation, Writing the Original Draft. E. Faizabadi: Supervision, Writing, Reviewing, and Editing.

References

[1] Xia, Y., Yang, P., Sun, Y., Wu, Y., Mayers, B., Gates, B., Yin, Y., Kim, F. and Yan, H., 2003. One-dimensional nanostructures: synthesis, characterization, and applications. *Advanced materials*, *15*(5), pp.353-389.

[2] Son, Y.W., Cohen, M.L. and Louie, S.G., 2006. Half-metallic graphene nanoribbons. *nature*, *444*(7117), pp.347-349.

[3] Song, Y.-L., Zhang, Y., Zhang, J.-M. and Lu, D.-B. J. a. S. S. 2010. Effects of the edge shape and the width on the structural and electronic properties of silicene nanoribbons. 256**,** 6313-6317.

[4] Lopez-Bezanilla, A., Huang, J., Terrones, H. and Sumpter, B.G., 2011. Boron nitride nanoribbons become metallic. *Nano letters*, *11*(8), pp.3267-3273.

[5] Kou, L., Tang, C., Zhang, Y., Heine, T., Chen, C. and Frauenheim, T., 2012. Tuning magnetism and electronic phase transitions by strain and electric field in zigzag MoS2 nanoribbons. *The journal of physical chemistry letters*, *3*(20), pp.2934-2941.

[6] Jiao, L., Zhang, L., Wang, X., Diankov, G. and Dai, H., 2009. Narrow graphene nanoribbons from carbon nanotubes. *Nature*, *458*(7240), pp.877-880.

[7] Tapasztó, L., Dobrik, G., Lambin, P. and Biro, L.P., 2008. Tailoring the atomic structure of graphene nanoribbons by scanning tunnelling microscope lithography. *Nature nanotechnology*, *3*(7), pp.397-401.

[8] Wang, X.H. and Zhou, Y.C., 2010. Layered machinable and electrically conductive Ti2AlC and Ti3AlC2 ceramics: a review. *Journal of Materials Science & Technology*, *26*(5), pp.385-416.

[9] Eklund, P., Beckers, M., Jansson, U., Högberg, H. and Hultman, L., 2010. The Mn+ 1AXn phases: Materials science and thin-film processing. *Thin Solid Films*, *518*(8), pp.1851-1878.

[10] Khazaei, M., Arai, M., Sasaki, T., Chung, C.Y., Venkataramanan, N.S., Estili, M., Sakka, Y. and Kawazoe, Y., 2013. Novel electronic and magnetic properties of two-dimensional transition metal carbides and nitrides. *Advanced Functional Materials*, *23*(17), pp.2185-2192.

[11] Zhao, S., Kang, W. and Xue, J., 2015. MXene nanoribbons. *Journal of Materials Chemistry C*, *3*(4), pp.879-888.

[12] Zhang, X., Zhao, X., Wu, D., Jing, Y. and Zhou, Z., 2015. High and anisotropic carrier mobility in experimentally possible Ti 2 CO 2 (MXene) monolayers and nanoribbons. *Nanoscale*, *7*(38), pp.16020-16025.

[13] Hong, L., Klie, R.F. and Öğüt, S., 2016. First-principles study of size-and edge-dependent properties of MXene nanoribbons. *Physical Review B*, *93*(11), p.115412.

[14] Giannozzi, P., Baroni, S., Bonini, N., Calandra, M., Car, R., Cavazzoni, C., Ceresoli, D., Chiarotti, G.L., Cococcioni, M., Dabo, I. and Dal Corso, A., 2009. QUANTUM ESPRESSO: a modular and open-source software project for quantumsimulations of materials. *Journal of physics: Condensed matter*, *21*(39), p.395502.

[15] Giannozzi, P., Andreussi, O., Brumme, T., Bunau, O., Nardelli, M.B., Calandra, M., Car, R., Cavazzoni, C., Ceresoli, D., Cococcioni, M. and Colonna, N., 2017. Advanced capabilities for materials modelling with Quantum ESPRESSO. *Journal of physics: Condensed matter*, *29*(46), p.465901.

[16] Giannozzi, P., Baseggio, O., Bonfà, P., Brunato, D., Car, R., Carnimeo, I., Cavazzoni, C., De Gironcoli, S., Delugas, P., Ferrari Ruffino, F. and Ferretti, A., 2020. Quantum ESPRESSO toward the exascale. *The Journal of chemical physics*, *152*(15).

[17] Kokalj, A., 2003. Computer graphics and graphical user interfaces as tools in simulations of matter at the atomic scale. *Computational Materials Science*, *28*(2), pp.155-168.

[18] Prandini, G., Marrazzo, A., Castelli, I.E., Mounet, N. and Marzari, N., 2018. Precision and efficiency in solid-state pseudopotential calculations. *npj Computational Materials*, *4*(1), p.72.

[19] Zhou, Y., Luo, K., Zha, X., Liu, Z., Bai, X., Huang, Q., Guo, Z., Lin, C.T. and Du, S., 2016. Electronic and transport properties of Ti2CO2 MXene nanoribbons. *The Journal of Physical Chemistry C*, *120*(30), pp.17143-17152.

[20] Yao, W., Yang, S.A. and Niu, Q., 2009. Edge states in graphene: From gapped flat-band to gapless chiral modes. *Physical review letters*, *102*(9), p.096801.

[21] Plotnik, Y., Rechtsman, M.C., Song, D., Heinrich, M., Zeuner, J.M., Nolte, S., Lumer, Y., Malkova, N., Xu, J., Szameit, A. and Chen, Z., 2014. Observation of unconventional edge states in 'photonic graphene'. *Nature materials*, *13*(1), pp.57-62.